



Parker, Max and Finney, Stephen and Holliday, Derrick (2017) DC protection of a multi-terminal HVDC network featuring offshore wind farms. Energy Procedia. ISSN 1876-6102 (In Press) ,

This version is available at <https://strathprints.strath.ac.uk/61162/>

Strathprints is designed to allow users to access the research output of the University of Strathclyde. Unless otherwise explicitly stated on the manuscript, Copyright © and Moral Rights for the papers on this site are retained by the individual authors and/or other copyright owners. Please check the manuscript for details of any other licences that may have been applied. You may not engage in further distribution of the material for any profitmaking activities or any commercial gain. You may freely distribute both the url (<https://strathprints.strath.ac.uk/>) and the content of this paper for research or private study, educational, or not-for-profit purposes without prior permission or charge.

Any correspondence concerning this service should be sent to the Strathprints administrator: strathprints@strath.ac.uk



9th International Conference on Applied Energy, ICAE2017, 21-24 August 2017, Cardiff, UK

DC protection of a multi-terminal HVDC network featuring offshore wind farms

Max Parker^{a*} Stephen Finney^a Derrick Holliday^a

^aUniversity of Strathclyde, Technology and Innovation Centre, 99 George St., Glasgow, G1 1RD, UK

Abstract

A protection scheme for DC faults has been designed for a multi-terminal HVDC network used to transfer energy from three large offshore wind farms to shore. The system uses open access models created in the EU-funded BEST-PATHS project, including a manufacturer-supplied wind farm model. Tripping conditions for the DC circuit breakers are found through simulation, along with current limiting inductor sizes, based on the use of a hybrid circuit breaker. Simulations of faults in the HVDC network show the ability of the protection scheme to isolate the fault, and the converter stations and wind turbines are able to ride-through the fault without tripping based on the 5ms switching time of the circuit breakers. Longer switching times will cause significant rises in the offshore grid frequency, which could cause the turbines to trip.

© 2017 The Authors. Published by Elsevier Ltd.

Peer-review under responsibility of the scientific committee of the 9th International Conference on Applied Energy.

Keywords: HVDC; Multi-terminal; DC protection; offshore wind

1. Introduction

In Europe wind energy, particularly generated offshore, is set to become an increasing part of the generation mix, due to the need to reduce carbon dioxide emissions and achieve security of supply. Significant investment in transmission infrastructure will be required to transmit the power to where it is required, as well as to transfer power around the continent to balance intermittent sources like wind and solar. It has been recognized that a business as usual approach will not be able to achieve the required interconnection at reasonable cost[1,2].

Most current offshore wind farms, of small size and close to shore, use high voltage AC transmission (HVAC) but increasing numbers are being planned with large capacities and located a significant distance from shore, making high

* Corresponding author. Tel.: +44-141-444-7328;

E-mail address: max.parker@strath.ac.uk

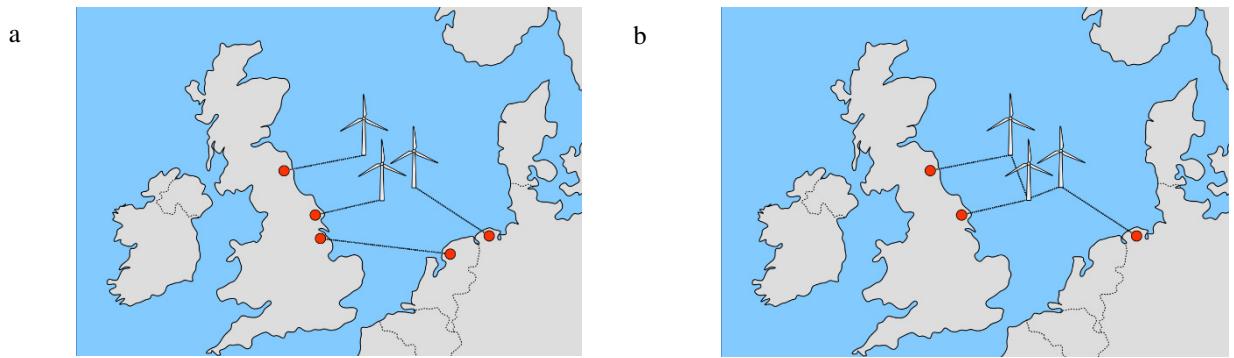


Fig. 1 Potential North Sea offshore wind connection, (a) point-point, (b) multi-terminal.

voltage DC (HVDC) transmission the most cost effective option. HVDC is also used for interconnection of un-synchronised grids, e.g. between the UK and European grids, and long undersea interconnections. These systems will use the newer voltage-source converter-based (VSC) HVDC, which allows a converter station sufficiently small to be located on an offshore platform and able to operate without a strong grid reference[3,4]. Multi-terminal HVDC (MTDC) has also been proposed as a way to reduce costs[5]. For instance, the point-point links in Fig. 1a could be replaced with the multi-terminal arrangement in Fig. 1, reducing the cable length and number of converter stations.

A significant issue relating to the use of HVDC in the connection of wind farms and in MTDC is a lack of experience in the industry with VSC-HVDC, particularly when used with offshore wind, although there have been many academic studies of this arrangement. Moreover, significant problems have been reported with the German BorWin1 HVDC link, which connects the BARD Offshore 1 windfarm to shore, including harmonic problems in the offshore grid potentially due to interactions between the converter station and wind turbines, and frequent outages, leading to significant compensation claims against the link operator[6,7]. Because of these issues other wind farm developers have been reluctant to invest in HVDC technologies, particularly MTDC.

The EU FP7 project BEST-PATHS was set up to reduce the technical barriers to the integration of large amounts of renewable energy production within Europe, and the consortium consists of transmission system operators, equipment vendors, and research organisations. Within the consortium, the Demo 1 partners have developed an open access MATLAB/Simulink toolbox for study of the integration of offshore wind farms using MTDC grids, including generic models of VSC stations based on modular multilevel converters (MMCs), frequency dependent DC cable models, high level controllers, and an aggregated wind farm model based on a real wind turbine design[8]. It is hoped that this toolbox will allow greater study of the interactions between offshore wind and HVDC systems, and with the AC grid, thereby reducing the risks in deploying such a system.

This paper presents work carried out DC protection of a multi-terminal HVDC network used to transmit offshore wind power to shore, carried out using the BEST-PATHS toolbox. This study differs from most others in that it includes multiple GW-sized wind farms connected to a multi-terminal link, an arrangement which could be used with some of the larger UK and German projects. Furthermore, this study uses a wind farm model based on a real turbine design, which is also significant as there are many conditions which could cause a real wind turbine to disconnect which may not be considered in a generic wind turbine model.

2. MTDC Network Configuration

The MTDC network used in this study is shown in Fig. 2, and is based on a proposal for the connection of a large UK Round 3 offshore wind farm. The wind farm is divided into three 1GW blocks, connected to shore with HVDC links operating at $\pm 320\text{kV}$ using 100km long XLPE cables. The offshore converter stations are then linked on the DC side using shorter cables. Each wind farm block has a single converter station, but uses four collector platforms, connected using 220kV AC cables, with a wind turbine collection network voltage of 33kV. For simplicity, each wind farm block is aggregated to a single wind turbine, lumped collection network cable capacitance, step-up transformer and 220kV cable. The HVDC converters are all of the half-bridge MMC type, with 320 modules per arm, rated at

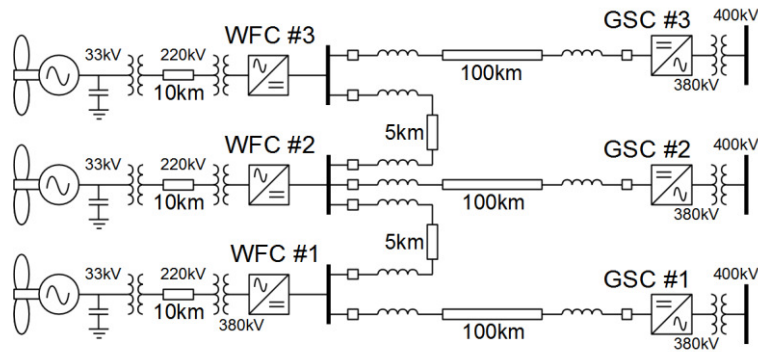


Fig. 2 MTDC Wind farm grid connection.

1GW. The 100km DC cables use a frequency-dependent travelling wave model, while the 5km DC and 10km AC cables use a pi-section model. The transformers used have a leakage reactance of 0.1pu, and the onshore grid has a short circuit ratio of 15. A more detailed description of the models used is provided elsewhere [8], and the toolbox can be freely downloaded from the BEST-PATHS website.

3. Design of the DC protection scheme

DC cable fault protection is achieved using DC circuit breakers at the ends of each cable, as shown in Fig. 2, along with inductors to aid fault discrimination and limit the fault current. A requirement placed on the DC protection scheme was that it must be able to isolate a fault within 6ms of the fault occurrence, and this requires the use of either hybrid or full semiconductor circuit breakers. The latter was rejected due to high losses, so a hybrid circuit breaker, of the type developed by ABB, was chosen, which is claimed to be able to isolate the circuit within 5ms, with a maximum breaking current of 10kA[9]. In normal use, current is conducted through a mechanical isolator and a low voltage semiconductor-based load commutation switch. In operation, the load commutation switch opens to divert the current through a semiconductor circuit breaker, the fast mechanical isolator then opens and finally the semiconductor circuit breaker opens, with the fault energy absorbed by metal oxide varistors. This circuit breaker design was modelled in Simulink, with the commutation of the current through the semiconductor breaker assumed to be instantaneous and the opening time of the fast isolator assumed to be 5ms. In addition to the circuit breakers, the converter stations will change to a blocking state if the DC current exceeds 4000A in order to protect the main switching devices, with current carried by the parallel diodes. The converter stations will de-block once the DC voltage has recovered above 500kV.

Research suggests that the derivative of DC current or voltage can be used to detect and locate a DC cable fault, with a low computational burden[10], so these methods are considered in this study. Therefore, the first task is to analyse the DC fault currents and voltages for a number of different fault locations, types and resistances to determine thresholds to trigger each circuit breaker. Following that, the size of the DC inductors must be set such that the fault current does not exceed the breaking capacity of the circuit breaker. Finally, the initial tests must be re-run in order to verify the tripping thresholds still apply with the revised inductances.

3.1. Circuit breaker trip threshold analysis

Simulations were carried out at multiple fault locations, with faults at either ends of the cables, and with fault resistances from 0.001-10 Ω , with both pole-ground and pole-pole faults considered. DC current and voltage at the circuit breaker positions were sampled at a rate of 10kHz, and the derivatives calculated. In these tests the current limiting inductors were set to 10mH.

For each circuit breaker location, DC current and voltage are plotted as well as their derivatives, with plots from all simulations overlaid on one graph. Plots are coloured to reflect whether or not the fault is in a cable adjacent to the

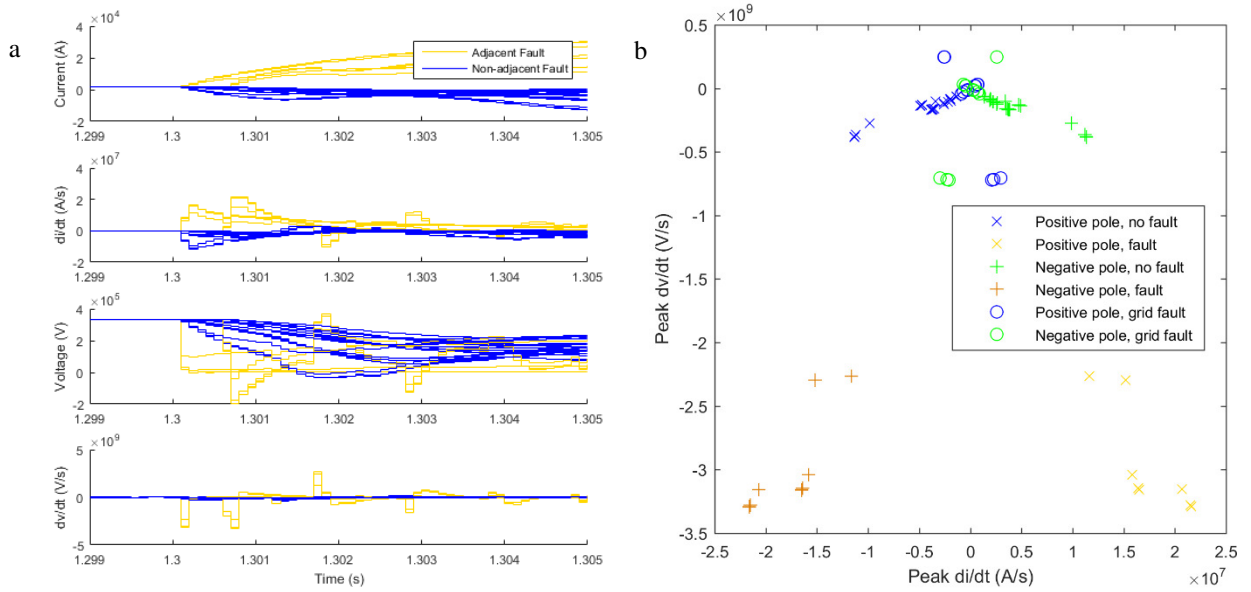


Fig. 3 Currents and voltages at one circuit breaker during DC cable faults. a) Time series, b) Peak current and voltage derivatives.

circuit breaker, determining whether the circuit breaker must trip. Representative results for one circuit breaker are shown in Fig. 3a, for pole-pole faults and showing only the positive pole. From these results, the peak current and voltage derivatives can be calculated, and these are shown for symmetrical faults in Fig. 3b. Also included are the peak current and voltage derivatives during AC grid faults in various locations, as these must not trigger the DC protection. From these results it appears that the voltage derivative gives the best detection margin, and in this case a threshold of -1.5GV/s is suitable. For pole-ground faults, the peak voltage and current derivatives on the faulted pole are similar, so the same threshold can be used – as the system is a symmetric monopole it cannot operate with one faulted pole, so a fault detection will cause both the positive and negative circuit breakers to trip.

3.2. Current limiting inductor size

Simulations were repeated with the fault resistance set at 0.001Ω , and this time with the current limiting inductance varied as well as the fault location. For each circuit breaker the fault conditions for which the circuit breaker would have to trip were selected and applied to time domain simulations using the previously-calculated voltage derivative

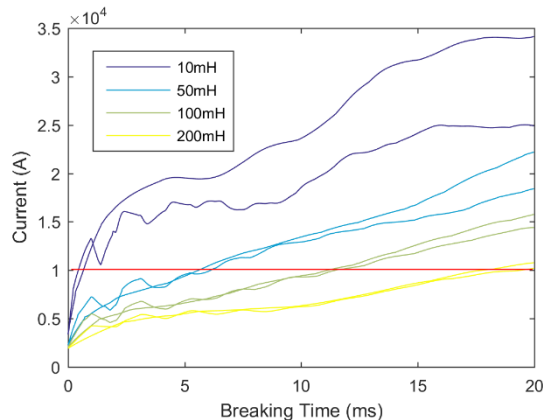


Fig. 4 Variation in breaking current with limiting inductor size.

thresholds to identify breaker trip time. Representative results for one circuit breaker are shown in Fig. 4, with zero time corresponding to the tripping instant for all curves. In the case illustrated it can be seen that a 50mH inductance may maintain the breaking current below 10kA for a 5ms breaking time. Similar studies over the whole network indicated a minimum inductance of 100mH to be required.

4. DC protection results and wind farm behavior

The response to a fault on the 100km DC cable close to WFC #3 is shown in Fig. 5 for pole-pole and pole-ground faults. As expected, the largest disturbances occur around GSC #3 and WFC #3, which are directly connected to the faulted cable, with the current limiting inductors ensuring that only GSC #3 sees sufficient overcurrent to block, with WFC #3 current limited by the offshore transformer reactances. The pole-ground fault leads to a greatly reduced overcurrent but significant over-voltages – the star points of the converter transformers are connected to ground with a high impedance to allow for over-modulation, but this prevents the converter limiting the overvoltage.

During a significant dip in the HVDC voltage, the wind farm HVDC converters will be unable to regulate the offshore voltage, whether blocked or not, and the turbines will effectively be islanded for the duration of the fault. The response of wind farm #3 is shown in Fig. 6a. The wind farm is unable to export real power, causing the turbine

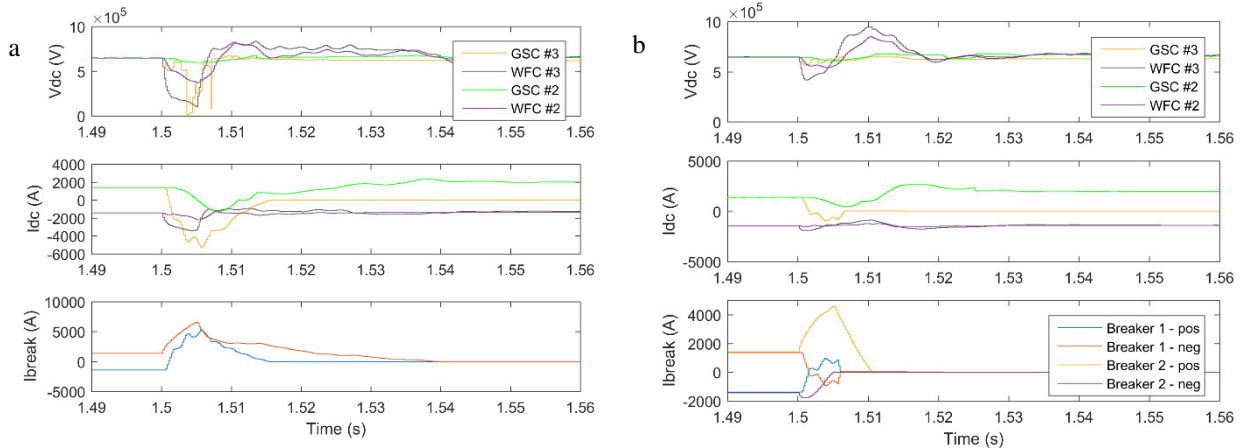


Fig. 5 Response to a DC cable fault, a) symmetrical fault, b) asymmetrical fault.

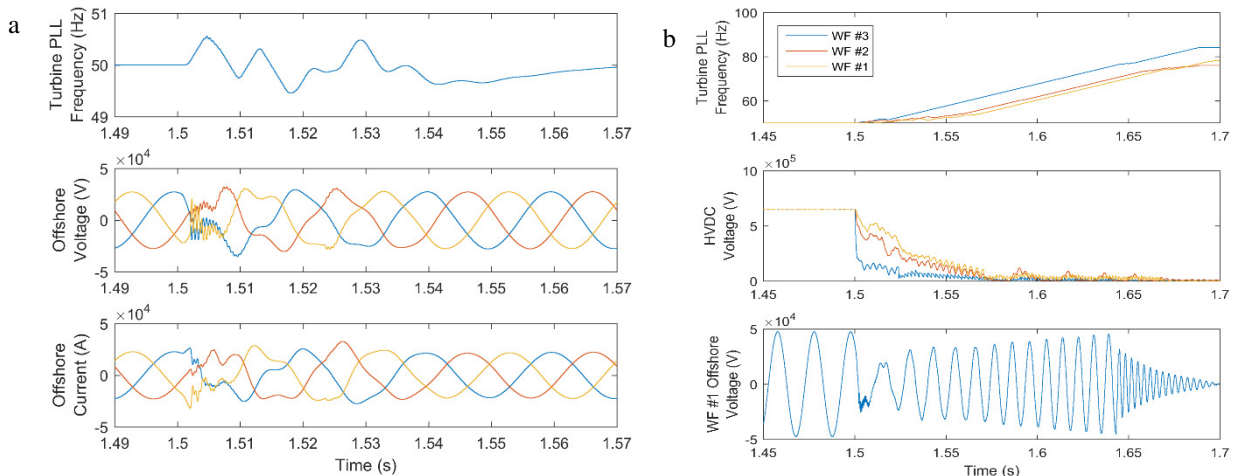


Fig. 6 Offshore grid behaviour during DC faults. a) 5ms breaking time, b) 20ms breaking time.

PLL frequency to increase, but this only lasts until the fault is cleared after 5ms, at which point the offshore terminal restores control and the turbine re-synchronises to the 50Hz reference, with some voltage distortion due to excitation of resonant frequencies in the offshore AC grid. The response if the circuit breakers do not operate is shown in Fig. 6b, in which the DC voltage collapses at all terminals, and the offshore network frequencies increase rapidly. Requirements for operating at high frequencies depend on the grid code, for instance the GB grid code allows but does not require disconnection if the frequency exceeds 52Hz, while the E.ON offshore grid code requires disconnection above 53.5Hz after a delay of 300ms. In this case the turbines are set to operate under the GB grid code, and will disconnect at 53Hz after a 500ms delay [11]. The reactive power supplied by the turbines is able to maintain the offshore grid voltage, but the turbines eventually disconnect around 140ms after the fault due to grid undervoltage – measurements of grid voltage are based on a fundamental frequency of 50Hz in accordance with IEC61400, and the increased frequency leads to an incorrect measurement.

5. Conclusion

A DC protection system based on hybrid circuit breakers has been devised and simulated for a multi-terminal HVDC network for connecting large offshore wind farms to shore. Behavior of the wind turbines and offshore grid have been modelled based on a manufacturer-supplied wind farm model, and the wind farm shown to be capable of riding through a HVDC fault based on a circuit breaker switching time of 5ms. Longer fault times may result from alternative protection schemes employing slower circuit breakers or de-energisation of the DC grid [12,13]. These will cause a significant rise in the offshore grid frequency, at a rate determined by the turbine PLL settings, and will eventually cause the turbine to disconnect through various mechanisms. Behavior in this islanded condition is generally not defined by the grid codes, and while this turbine could handle a DC fault of over 100ms, such operation is not guaranteed for all models of turbine.

Acknowledgements

This project was supported by the EU FP7 program, through the project “BEYOND State of the art Technologies for re-Powering AC corridors and multi-Terminal HVDC Systems” (BEST-PATHS), grant number 612748. The simulation toolbox can be downloaded from the project website at www.bestpaths-project.eu.

References

- [1] European Commission (EC), “Transmission system operation with large penetration of Wind and other renewable Electricity sources in Networks by means of innovative Tools and Integrated Energy Storage (TWENTIES)”, 2014.
- [2] NorthSeaGrid, “NorthSeaGrid: Integrated Offshore Grid Solutions in the North Sea”, Policy Brief, 2015.
- [3] V. Hussennether et. al., “Projects BorWin2 and HelWin1 – Large Scale Multilevel Voltage-Sourced Converter Technology for Bundling of Offshore Windpower,” CIGRE Session, Paris, 2012.
- [4] L. Xu, B. R. Andersen, “Grid Connection of Large Offshore Wind Farms Using HVDC,” *Wind Energ.* Vol. 9, pp. 371–382, 2006.
- [5] O. Gomis-Bellmunt et. al., “Topologies of multiterminal HVDC-VSC transmission for large offshore wind farms,” *Electric Power Systems Research*, vol. 81, pp. 271–281, 2011.
- [6] ‘Analysis: Bard1 transmission problems could prompt payout,’ *Windpower Offshore*, 18th June 2014, Available online at www.windpoweroffshore.com/article/1299358
- [7] ‘Dirty electricity probe at BorWin1,’ *reNEWS*, 11th June 2014, Available online at renews.biz/68145
- [8] C. Ugalde-Loo et. al., “Open access simulation toolbox for the grid connection of offshore wind farms using multi-terminal HVDC networks,” 13th IET Int. Conf. on AC and DC Power Transmission, Manchester, 2017.
- [9] M. Callavik et. al., “The Hybrid HVDC Breaker: An innovative breakthrough enabling reliable HVDC grids,” Tech. Paper, ABB Grid Systems, 2012.
- [10] J. I. Marvik, S. D’Arco, J. A. Suul, “Communication-less fault detection on radial multi-terminal offshore HVDC grids,” 11th IET Int. Conf. on AC and DC Power Trans., Birmingham, 2015.
- [11] M. Tsili, S. Papathanassiou, “A review of grid code technical requirements for wind farms,” *IET Renew. Power. Gener.*, Vol. 3 (3), 2009.
- [12] F. Page, S. Finney, L. Xu, “An Alternative Protection Strategy for Multi-terminal HVDC,” 13th Wind Integration Workshop, Berlin, 2014.
- [13] J. Candelaria, J. Park, “VSC-HVDC System Protection: A Review of Current Methods,” *IEEE/PES Power Syst. Conf. and Expo. PSCE2011*.